· Article ·
doi: 10.13679/j.advps.2016.1.00039

Advances in Polar Science
March 2016 Vol. 27 No. 1: 39-47

Structure and seasonal variability of fronts in the Southeast Indian Ocean along sections from Fremantle, Australia to Antarctic Zhongshan Station

YANG Wei[1,2,3], GAO Libao[4], LI Ruixiang[1], LIU Changjian[1] & YAN Jinhui[1*]

[1] South China Sea Marine Survey and Technology Center, State Oceanic Administration, Guangzhou 510300, China;

[2] State Key Laboratory of Tropical Oceanography, South China Sea Institute of Oceanology, Chinese Academy of Sciences, Guangzhou 510301, China;

[3] University of Chinese Academy of Sciences, Beijing 100049, China;

[4] First Institute of Oceanography, State Oceanic Administration, Qingdao 266061, China

Received 12 January 2016; accepted 30 March 2016

Abstract Four sections of expendable conductivity-temperature-depth (XCTD) profiles from Fremantle, Australia to Antarctic Zhongshan Station and Moderate Resolution Imaging Spectroradiometer-Aquarius (MODIS-A) sea surface temperature (SST) products were used to study the structure and seasonal variability of Southeast Indian Ocean fronts. Water mass analysis showed that surface water masses in the Southeast Indian Ocean were less salty in March than in November. Compared with November, the subtropical front (STF) moved southward about one degree of latitude in March, whereas seasonal variability of the subantarctic front (SAF) and polar front (PF) locations was not obvious. In March, the saline front moved northward about two degrees of latitude relative to the thermal front in the upper 100 m at the SAF, which was the northern boundary of sub-Antarctic surface water (SASW). Analysis of climatological SST gradients from the satellite data showed that regions of enhanced sea surface temperature (SST) gradients were collocated with frontal locations identified with the XCTD data using water mass criteria. The surface expression of the PF identified by the SST gradient was further south by about one degree of latitude relative to the subsurface expression of the PF identified by the northern boundary of cold water.

Keywords **Southeast Indian Ocean, ocean fronts, XCTD, satellite sea surface temperature, seasonal variability**

Citation: Yang W, Gao L B, Li R X, et al. Structure and seasonal variability of fronts in the Southeast Indian Ocean along sections from Fremantle, Australia to Antarctic Zhongshan Station. Adv Polar Sci, 2016, 27: 39-47, doi: 10.13679/j.advps.2016.1.00039

1 Introduction

The Southern Ocean is the broad ocean region surrounding Antarctica, and is a collective name for the southern Pacific, southern Atlantic, and southern Indian Ocean. Therefore, it is not a formal geographic region. Because there is no north-south boundaries in the latitude range of the Drake Passage, the strong Antarctic Circumpolar Current (ACC) flows continuously eastward. ACC transport is >100 Sv (1 Sv= 10^6 $m^3 \cdot s^{-1}$)[1]; thus, it plays a crucial role in the global transport of mass, heat and momentum, and has a deep impact on global climate change[2]. The most striking feature of the Southern Ocean is its separation by different zonal fronts, and zones between these fronts have homogeneous water masses[2-3].

The structure and variability of the major fronts in the Southern Ocean have been studied for many years. By synthesizing all historical *in situ* hydrographic data[2–8] and recent Argo profiles[6], the distribution of mean locations and vertical structures of Southern Ocean fronts could be depicted. Among these, the climatological frontal patterns of Belkin and Gordon[3] and Orsi et al.[2] were the most prominent and

* Corresponding author, E-mail: yanjinhui@smst.gz.cn

most widely applied by other studies. Another important and effective way to collect *in situ* temperature and salinity profiles was the launch of expendable bathythermography (XBT)/expendable conductivity-temperature-depth (XCTD) probes along the cruise tracks of supply ships, and the structure of major fronts in the upper layer above 1000-meter depth in the Southern Ocean had been well described[8–13]. In the Southeast Indian Ocean sector where the Antarctic Zhongshan Station was located, locations and typical vertical structures of major fronts, including the subtropical front (STF), subantarctic front (SAF), polar front (PF), southern ACC front (SACCF), and Antarctic slope front (ASF), were clearly identified according to criteria based on water mass[2-3,7,9–13]. The fronts encircling Antarctica as parts of the ACC were the SAF, PF, and SACCF. Within the fronts, the currents were strong and eastward[2,6,8].

Owing to the remote location and harsh weather conditions, *in situ* observations in the Southeast Indian Ocean were sparse and discontinuous, which had prevented us from understanding seasonal and interannual variability of the fronts. Satellite data could solve this problem. Long time series of sea surface height (SSH) observations had been used in a number of studies to detect the fronts and compare with frontal positions inferred from hydrographic sections using traditional water mass criteria[8,15–18]. Next, SSH products were used to study the dynamical and temporal variability of major fronts[14–21]. Recently, increased attention had been given to satellite sea surface temperature (SST) products[15,22–27,29-30], especially using SST gradients to identify the PF[24-25,27,29-30]. Various SST products, such as the AVHRR SST for long time series[24–26] and AMSR-E satellite SST for cloud-penetrating radiometers[27–30], and various criteria[25–27,29] of front detection were used to identify the location and intensity of ocean fronts. Validation of frontal positions, inferred from SST gradients with the frontal pattern identified based on hydrographic surveys in previous works, had also been pursued[26,28–29]. The path, width and intensity of fronts were strongly influenced by topography[6,15,19,25,27]. In summer, frontal locations in the Southeast Indian Ocean extended further south than their long-term mean distribution as compared with winter[21], and a southward drift of ACC fronts had been indicated over the past 20 years[18,21].

Satellite data have had an irreplaceable role in seasonal variability study of major fronts in the Southeast Indian Ocean, but had mainly focused on the variability of location and intensity[18,20-21,26-27]. The vertical structure of fronts could only be described by *in situ* observations. Compared with the Drake Passage[2,4] and the section between Tasmania, Australia and Antarctica[2-4,8], repetition of the hydrographic section in the Southeast Indian Ocean was rare, except for tracks of supply ships. Zhongshan Station (69°22'S, 76°23'E) was established in 1989 at Prydz Bay, Antarctica. After that, underway XBT/XCTD sampling in the Southeast Indian Ocean along *R/V XUE LONG's* cruise tracks had shown to be a cost-effective means of collecting temperature and salinity profiles in this area. Based on repeat sections from Fremantle, Australia to Zhongshan Station in different months of a year, study of the seasonal variability of fronts not only focused on location and intensity, but also addressed the vertical structure variability of thermal and saline fronts.

In this paper, four XCTD sections during the 29th through 31st Chinese National Antarctic Research Expedition (CHINARE) were first used to study the structure and seasonal variability of fronts in the Southeast Indian Ocean. Then, Moderate Resolution Imaging Spectroradiometer-Aquarius (MODIS-A) SST products were validated with *in situ* observation data. Finally, the SST products were used for further analysis of frontal seasonal variability.

2 Data

Four XCTD sections from Fremantle, Australia to Zhongshan Station were executed during 20–27 November 2012, 22–26 November 2013, 1–10 March 2014, and 9–15 March 2015 (Figure 1). A total of 96 temperature and salinity profiles were collected. Spatial resolution of the XCTD samples

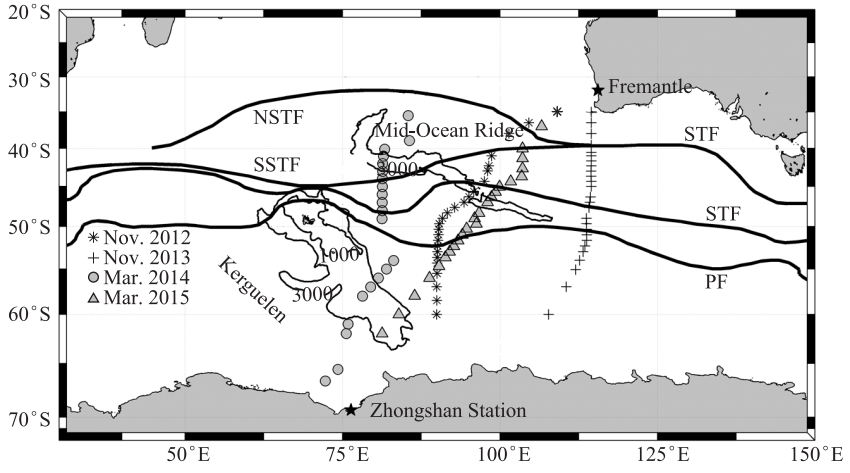

Figure 1 XCTD sampling locations in Southeast Indian Ocean. There were 25(26) samples in November 2012(2013), and 21(24) samples in March 2014(2015). The frontal patterns (bold black lines) in the Southeast Indian Ocean were taken from Belkin and Gordon[3] in 1996.

was about 40 minutes in latitude (minute: 1/60 of a degree) between 40°S and 60°S.

The device used on our cruises was a TSK XCTD-1. Specifications of this type of XCTD include the following: Temperature range –2°C to 35°C and accuracy ±0.02°C; conductivity range 20–74 mS·cm^{-1} and accuracy ±0.03 mS·cm^{-1}. The depth range was 1000 m at the rated vessel speed of 12 knots. Because the speed for *XUE LONG* was 14–16 knots when it crossed the Southeast Indian Ocean, we took the upper 900 m of data for analysis.

All XCTD profiles went passed through careful quality control. First, raw data were directly abandoned in the case of an obviously faulty probe, such as constant temperature and salinity, a broken wire, and data deficiency over a large depth range. Second, temperature and conductivity spikes caused by external electronic interference were removed from profiles, and the data gaps were filled by linear interpolation. Then, the raw data were saved at 1-m intervals by taking the average of all such data between half a meter above and below the integer meter. Finally, the 1-m interval data were smoothed for presentation in figures.

The 4-km, 8-day, and climatological monthly MODIS-ASST products (http://oceandata.sci.gsfc.nasa.gov/MODISA/Mapped/) were also used in analyses of frontal seasonal variability across the Southeast Indian Ocean.

3 Water masses and T/S structures

Water masses in the Southern Ocean could be considered to be in four layers: surface/upper Ocean, intermediate, deep, and bottom waters. These were mostly identified by salinity, potential temperature, and potential density[1]. In this paper, we focused on surface/upper ocean waters analysis, because only upper 900 m data were collected during the cruises. The four XCTD sections crossed three very different oceanic domains, i.e., the subtropical gyre, subantarctic region, and polar ocean, so water mass characteristics were distinct.

Data from all four cruises were selected for comparison (Figure 2), red lines were November 2012 and 2013, blue lines were March 2014 and 2015. According to the conventions for naming water masses in earlier studies (Table 1), water masses observed were: subtropical surface water (STSW), located north of the STF; subantarctic mode water (SAMW), which is identified in the subsurface as a vertically uniform layer from 40°S to 45°S; subantarctic surface water (SASW), located south of the SAF and north of the PF; Antarctic surface water AASW, located south of the PF and above upper circumpolar deep water (UCDW).

The minimum salinty of STSW was ~34.9 in March and ~35.1 in November. Minimum salinity of SASW was ~33.75 in March and ~34 in November. The salinities of AASW and UCDW in March were less than in November. Water with salinity < 33 was observed during March in the area south of 65°S. SAMW water properties were stable, with no obvious seasonal variability. The Southern Ocean was dominated by westerlies in the latitude band 40°S–60°S[2]. The less salty surface water masses in March resulted from melted sea ice driven northward to a more extensive Southern Ocean by the westerlies after summer.

4 Structure and seasonal variability of fronts in Southeast Indian Ocean

Oceanic fronts were important features in the Southern Ocean, and were identified by sharp horizontal water property contrasts between water masses[1]. Many studies

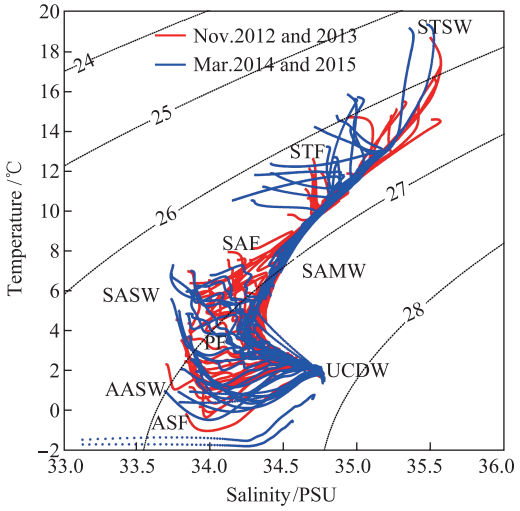

Figure 2 T/S plot based on data collected in November 2012 and 2013, March 2014 and 2015.

Table 1 Definition of water masses

Water mass	Definition	Reference
STSW	Relatively high temperature (>12°C) and salinity (>35.1)	Park et al.[31]
SAMW	Vertically uniform water with density between 26.90 and 26.95 located above 450–600 dbar	Yuan et al.[10]; Rintoul and Bullister[4]
SASW	Temperature between 5°C–9°C and salinity less than 34	Talley et al.[1]; Yuan et al.[10]; Park et al.[31]
AASW	Temperature below 2°C and salinity lower than 34.1	Yuan et al.[10]; Rintoul and Bullister[4]
UCDW	Below AASW, upper layer of the warm and saline water mass occupied most of the deep layers of the ACC	Orsi et al.[2]; Park et al.[31]; Rintoul and Bullister[4]

had used different criteria to identify frontal positions[2-3,10,12,31]. In this paper, we focused on frontal characteristics in the Southeast Indian Ocean. In order to compare with the conclusions of pervious studies, the criteria from Belkin and Gordon[3] in 1996 was used. Orsi et al. pointed out that the SAF is the northern edge of the ACC, whereas the SACCF was the dynamical southern boundary of the ACC[2]. We also describe the SACCF location according to our observation data.

The STF was identified by the 12°C isotherm at 200 m depth, with a maximum gradient between the 13°C and 15°C isotherms at the surface, and surface water salinity between the 34.9 and 35.5 isohalines[3,10]. The SAF could be identified by a maximum gradient between the 4°C and 8°C isotherms, and the 34.1 and 34.5 isohalines at 200-m depth[3,10,31]. The PF could be identified by the northernmost location of the 2°C isotherm surrounding the temperature minimum layer[2,3,10]. Yuan et al. stated that the location where isotherms were between 3 and 6°C with a strong gradient might also be identified as the PF[10]. The SACCF could be identified by temperature <0°C at depths shallower than 150 m, or temperature >1.8°C at depths greater than 500 m[2]. Flow at the ASF was westward, and was mainly characterized by a pycnocline that angles downward toward the continental slope. The ASF separates cold, dense waters from offshore surface water masses that were always located south of 60°S[2,32].

4.1 Cruises during November in 2012 and 2013

According to the aforementioned criteria, the structure and location of fronts during November could be identified. XCTD sampling locations were between 90°E and 100°E during November 2012 (Figure 1). Section distributions of temperature and salinity were presented in Figures 3a and 4a. The STF was around 39.5°S, where the 13°C isotherm and 35.5 isohaline were, and the depth range, as defined by 12°C isotherm and 34.8 isohaline, was ~250 m. The SAF was around 45.0°S, where the 6–9°C isotherms and 34.2–34.7 isohalines had a strong horizontal gradient, and the depth range was across the entire observation layer. The PF was around 53.5°S, the northernmost extent of the 2°C isotherm. There were strong horizontal gradients between the 4–7°C isotherms and 34.2–34.4 isohalines around 47.5°S and 50.0°S, respectively. According to the criteria, these could be identified as two other PFs. The SACCF was south of 57°S, where the temperature was < 0°C at 100-m depth.

The XCTD sampling locations were between 107°E and 114°E in November 2013 (Figure 1). Section distributions of temperature and salinity were shown in Figures 3b and 4b. The double structure of the STF could be observed along this section. The NSTF was around 37.5°S, where the 14°C isotherm and 35.2 isohaline were, and the depth range, as defined by 12°C isotherm and 34.8 isohaline, was greater

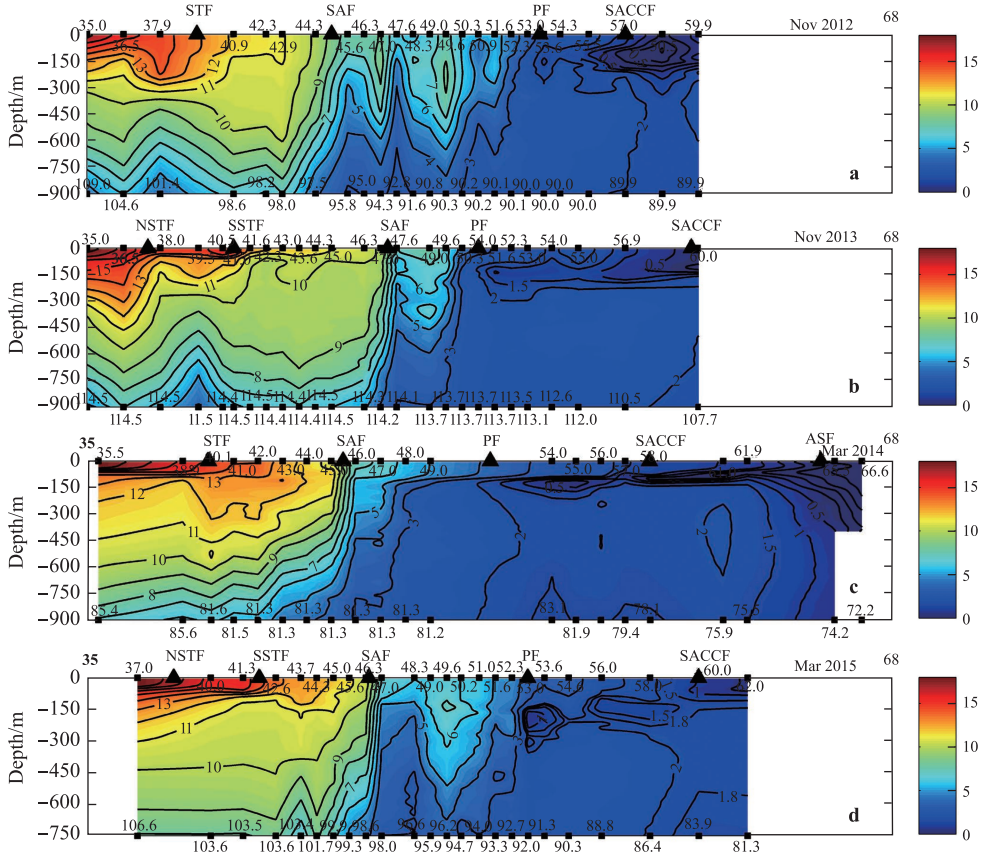

Figure 3 Temperature distribution along Fremantle/Zhongshan Station transect during November 2012 (**a**), November 2013 (**b**), March 2014 (**c**), and March 2015 (**d**).

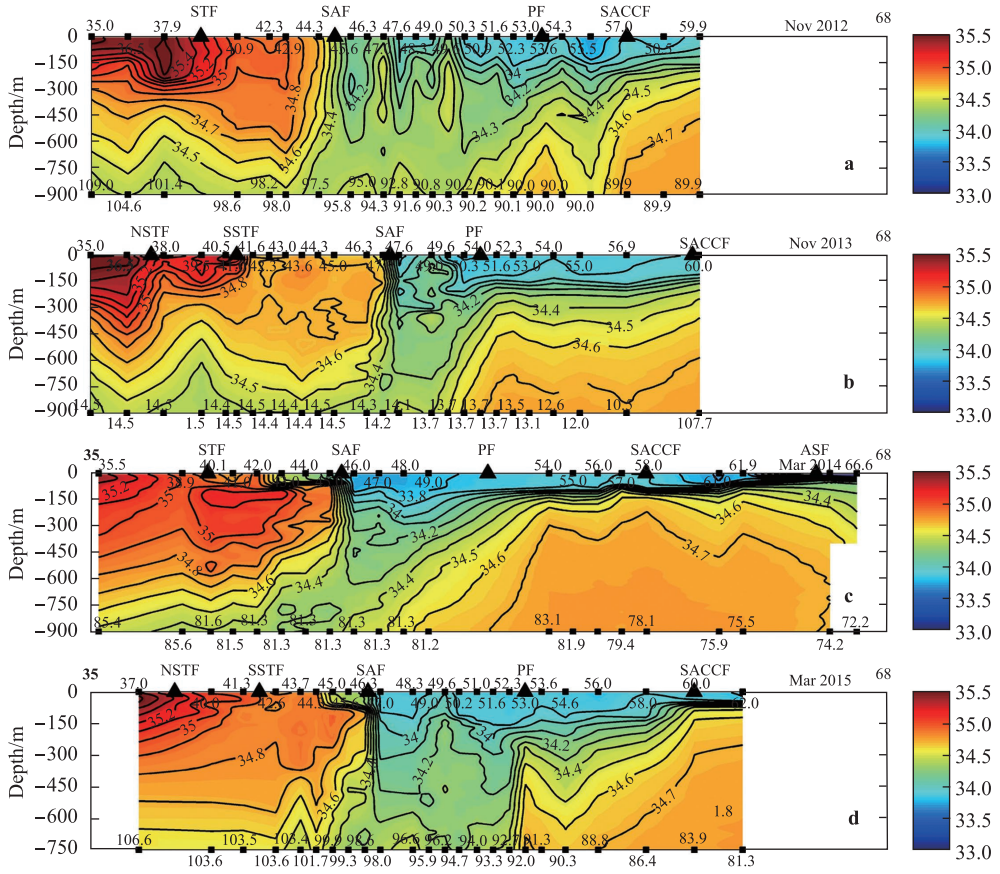

Figure 4 Salinity distribution along Fremantle/Zhongshan Station transect during November 2012 (**a**), November 2013 (**b**), March 2014 (**c**), and March 2015 (**d**).

than 400 m. The SSTF was around 41.0°S, where the 13°C isotherm and 35.0 isohaline were, and the depth range was only 150 m. The SAF was around 47.3°S, where the 6–9°C isotherms and 34.3–34.6 isohalines had a stronger horizontal gradient than in November 2012. The depth range again encompassed the entire observation layer. The PF was around 51.0°S, the northernmost extent of the 2°C isotherm. There was a strong horizontal gradient between the 3°C and 6°C isotherms and 33.9–34.1 isohalines, located around 50.0°S in the upper 200-m layer. The SACCF was around 60°S, where the temperature was < 0°C at 100-m depth.

4.2 Cruises during March in 2014 and 2015

XCTD sampling locations were between 72°E and 85°E in March 2014 (Figure 1). Section distributions of temperature and salinity were presented in Figures 3c and 4c. The STF was around 40.0°S, where the 15°C isotherm and 35.1 isohaline were, and the depth range, as defined by 12°C isotherm and 34.8 isohaline, was shallower than 200 m. The depth range and salinity of STSW were less than observed in November. The SAF was around 45.5°S, where the 5–9°C isotherms and 34.3–34.7 isohalines were. The saline front in the upper 100-m layer moved northward about three degrees of latitude to ~42.5°S, different from the saline front in November. The PF was around 51.5°S. The SACCF was around 58°S, where the temperature was <0°C at 100-m depth. The ASF was south of 65°S, where the 0.5–1.5°C isotherms were, with a maximum horizontal gradient in the subsurface layer.

XCTD sampling locations were between 80° and 105°E in March 2015 (Figure 1). Section distributions of temperature and salinity were shown in Figures 3d and 4d. The double structures of the STF could be identified from the temperature distribution. The NSTF was around 38.5°S, where the 17°C isotherm and 35.3 isohaline were. The SSTF was around 42.0°S, where the 13°C isotherm and 34.9 isohaline were, and the depth range, as defined by 12°C isotherm and 34.8 isohaline, was < 200 m. The SAF was around 46.5°S, where the 5–9°C isotherms and 34.3–34.7 isohalines were with a strong horizontal gradient. The saline front in the upper 100-m layer moved northward about two degrees of latitude to ~44.5°S, the same frontal structure as in March 2014. The PF was around 53.0°S, the northernmost extent of the 2°C isotherm. There was a water mass with high temperature and low salinity around 50.0°S in the upper 600-m layer. The SACCF was around 60°S, where the temperature was >1.8°C at depths >500 m.

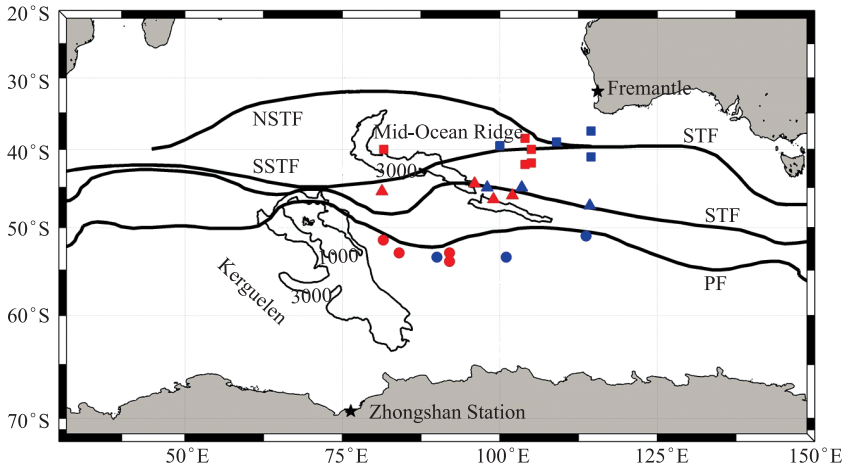

Figure 5 Location of STF (squares), SAF (triangles) and PF (circles) derived from cruises in March (red) and November (blue) from Table 2, superimposed on frontal pattern in the Southeast Indian Ocean from Belkin and Gordon[3] in 1996.

Table 2 Location comparison of Southeast Indian Ocean fronts in various years

	Nov. 1998 [10]	Nov. 2012	Nov. 2013	Mar. 2000 [10]	Mar. 2002 [10]	Mar. 2014	Mar. 2015
STF	39.0°S 109.0°E	39.5°S 100.0°E	37.5°S(N) 41.0°S(S) 114.5°E	41.8°S 105.0°E	40.0°S 105.0°E	40.0°S 81.6°E	38.5°S(N) 42.0°S(S) 104.0°E
SAF	45.0°S 103.5°E	45.0°S 98.0°E	47.3°S 114.3°E	44.5°S 96.0°E	46.0°S 102.0°E	45.5°S 81.3°E	46.5°S 99.0°E
PF	53.5°S 101.0°E	53.5°S 90.0°E	51.0°S 113.7°E	53.0°S 84.0°E	54.0°S 92.0°E	51.5°S 81.5°E	53.0°S 92.0°E
SACCF	/	57.0°S 90.0°E	60.0°S 110.0°E	/	/	58.0°S 80.0°E	60.0°S 84.0°E

Note: N/S in STF column indicates NSTF/SSTF

Table 3 Statistical Analysis of Southeast Indian Ocean fronts in various years

	Nov. 2012		Nov. 2013		Mar. 2014		Mar. 2015	
	Max-d/m	Max△T/°C·(100 km)$^{-1}$	Max-d/m	Max△T/°C·(100 km)$^{-1}$	Max-d/m	Max△T/°C·(100 km)$^{-1}$	Max-d/m	Max△T/°C·(100 km)$^{-1}$
STF	300	1.0	400	2.3	100(T) 300(S)	1.2	150(T) 300(S)	1.9
SAF	900(T) 800(S)	3.9	900(T) 700(S)	5.9	800(T) 500(S)	5.4	750(T) 450(S)	5.7
PF	/	2.2	/	1.8	/	1.4	/	4.9

Notes: Max-d indicates depth range of front; T/S stands for temperature/salinity; Max△T symbolizes maximum temperature gradient

4.3 Seasonal variability of fronts in Southeast Indian Ocean

Tables 2 and 3 compared the major fronts in the Southeast Indian Ocean in different years. Figure 5 presented the locations of the major fronts in Table 2 compared with the frontal pattern in the Southeast Indian Ocean given in Belkin and Gordon[3]. Together with the aforementioned section distributions (Figures 3 and 4), we could determine the structure and seasonal variability of the major fronts in the Southeast Indian Ocean.

The STF location in March was farther south by about one degree latitude relative to that in November. This characteristic persisted during the two cruises when the double STF structures were observed. The location of the NSTF (SSTF) in March 2015 was farther south by one degree of latitude relative to that in November 2013. Kim and Orsi also concluded that frontal locations in the Southeast Indian Ocean extended farther south in summer, by analyzing long time series of satellite SSH data[21]. The STF during these seven cruises in Table 2 was southward by about two degrees of latitude compared with the STF frontal pattern in Figure 5. The depth range of the STF in November was larger than that in March. The STF depth range was 300 m in November 2012, and the NSTF depth range was 400 m in November 2013. There was no obvious difference between

the structure of the thermal front and saline front. The depth range of the thermal front structure of the STF in March 2014 and 2015 was only 150 m. The depth range of the saline front reached ~300 m. The depth range difference between the thermal and saline front was also observed in March 2000 and 2002[10,12]. The maximum temperature gradient of the STF was ~1.0–2.0°C·(100 km)$^{-1}$.

The SAF gradient was the strongest compared with other major fronts in the upper 900 m. The maximum temperature gradient was >5.0°C·(100 km)$^{-1}$. The depth range of the thermal front encompassed the entire observation depth. The depth range of the saline front in March 2014 and 2015 was 500 m and 450 m, respectively, which was obviously shallower than the thermal front. The depth where horizontal salinity gradients weakened was the level at which Antarctic Intermediate Water spread northward[33]. The saline front moved northward about two degrees of latitude in the upper 100-m layer. This structural distribution of the saline front was also observed in March 2000 and 2002[10,12]. The SAF was the northern boundary of the ACC, which was the intersection area of the SASW and SAMW[1]. The northward extension of the saline front in the surface layer showed the influence of melted sea ice in March. There was no obvious seasonal variability in the SAF location which was 45°S–46°S in the sector 80°–105°E. This was consistent with the SAF frontal pattern in Figure 5. The SAF location was at 47.3°S along 114°E in November 2013. This showed that the latitudinal location of the SAF became more southerly upon moving from west to east across the Southeast Indian Ocean. This was evident in the frontal pattern of Belkin and Gordon in 1996 (Figure 5); the mean path of the SAF was believed to be strongly influenced by the bottom topography of the mid-ocean ridge[3,7,31].

The PF location in Tables 2 and 3 was the northernmost extent of the 2°C isotherm surrounding the minimum temperature layer. The PF location was stable at 53°S–54°S in the sector 80°E–105°E, which was southward by about one degree of latitude compared with the PF frontal pattern in Figure 5. Although the distance between the two sections in November 2013 and March 2014 was >30° in longitude, the PF location during those two cruises was ~51°S. This was northward by about two degrees of latitude compared with other cruises. The reason for this required further study. The maximum temperature gradient was ~1.4–2.0°C·(100 km)$^{-1}$ in the upper 300 m, which was closer to that of the STF and much less than that of the SAF. The location of the SACCF varied between the four cruises, and was 57°S–60°S in the sector 80°E–110°E. Because the SACCF was the dynamical southern boundary of the ACC, the difference of SACCF locations might show the variability of the ACC.

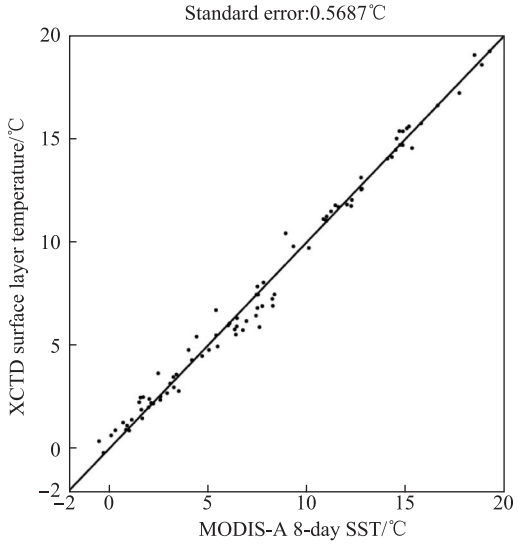

Figure 6 Comparison between MODIS-A 8-day SST and surface temperature from XCTD observations.

5 Seasonal variability of major fronts derived from satellite SST

5.1 Validation of MODIS-A SST products

To evaluate the performance of the MODIS-A SST products in the Southeast Indian Ocean, we took the average temperature of the upper 5-m layer as the observed surface temperature for each XCTD sampling station. Corresponding 8-day MODIS-A SST products of 16–23 November 2012, 24 November to 1 December 2012, 17–24 November 2013, 25 November to 2 December 2013, 26 February to 5 March 2014, 6–13 March 2014, 6–13 March 2015, and 14–21 March 2015 were selected for satellite SST calculation. All valid SST pixels in a 20 km × 20 km box where the XCTD sampling station was centered (resolution 4 km, 6 pixels × 6 pixels; 36 pixels in total) were averaged as the satellite SST value at each station. Figure 6 compared the MODIS-A 8-day SST and surface layer temperature from XCTD. There

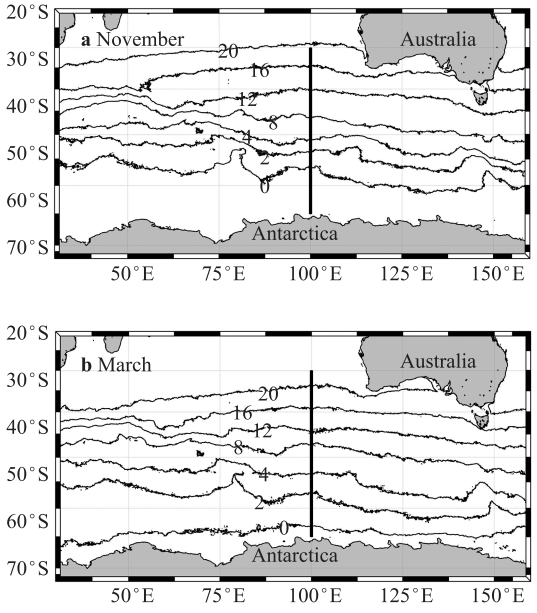

Figure 7 Climatological MODIS-A SST distribution in November (**a**) and March (**b**). The sea surface temperature gradient along 100°E (black vertical line) was calculated and presented in Figure 8.

were no corresponding satellite SST values for nine XCTD stations, and the standard error for the other 87 stations was 0.5687°C. The MODIS-A SST products showed excellent performance in the Southeast Indian Ocean.

5.2 Seasonal variability of major fronts in Southeast Indian Ocean

Figure 7 depicted the climatological November and March MODIS-A SST distributions in the Southeast Indian Ocean. November was spring and March was fall in the Southern Hemisphere, and the isotherms moved southward clearly after the summer.

To compare seasonal variability of major fronts in the Southeast Indian Ocean derived from the MODIS-A SST products, we calculated the climatological temperature gradient along 100°E longitude for March and November (Figure 8). All valid SST pixels within 0.5° latitude were averaged first, then temperature change every 100 km was calculated as the gradient for comparison. The STF was around 38.5°S and the temperature gradient was 0.9°C ·(100 km)$^{-1}$ in November. This front moved southward to ~40.5°S in March, and the temperature gradient was 1.2°C·(100 km)$^{-1}$. The location for the front moved southward about two degrees in latitude, consistent with the conclusion from XCTD observation. We also marked STF locations in Figure 8 for November 2012 and March 2015, when the XCTD sampling stations were near 100°E. STF locations during those two cruises were consistent with the enhanced SST gradient. The temperature gradient of the SAF was strongest along the 100°E section, at 1.8°C·(100 km)$^{-1}$. The SAF location was 45.5°S–46.5°S, also consistent with XCTD observations from November 2012 and March 2015. Surface-layer temperature was 8°C, consistent with the conclusion of Lutjeharms and Valentine[23], and there was no obvious seasonal difference in frontal position during March and November. The PF was around 54°S–54.5°S. The temperature gradient was 0.8°C·(100 km)$^{-1}$, smaller than the criteria for the PF (1.0–1.5°C·(100 km)$^{-1}$) provided by Dong et al.[27]. The PF was around 53°S–54°S, according to the criterion of the northernmost location of the 2°C isotherm. PF locations in November 2012 and March 2015 were also marked in Figure 8. This was northward by about one degree in latitude

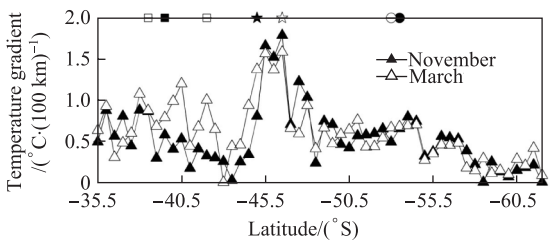

Figure 8 Climatological MODIS-A SST gradient along 100°E in March and November. Solid squares/pentagrams/circles show locations of the STF/SAF/PF in March 2015, and open squares/pentagrams/circles locations of the SSTF/NSTF/SAF/PF in November 2012.

compared with the frontal position derived from the satellite SST. Many studies had mentioned the difference between the surface and subsurface expressions of the PF[25,27,29-30]. The surface expression of the PF identified by the temperature gradient was farther south than the subsurface expression, identified by the northernmost extent of the 2°C isotherm. This difference was about 1 or 2 degrees of latitude in the conclusion of Moore et al.[25]. There was a relatively strong temperature gradient about 56°S–57°S in both March and November climatological data, which could reflect the surface expression of the SACCF.

The distribution of major fronts along 100°E was typical in the Southeast Indian Ocean. Seasonal variability of the major fronts could be identified clearly by the temperature gradient curves, and this was also consistent with the conclusions derived from the XCTD observations. The MODIS-A SST products can thus be used for seasonal variability analysis of the major fronts across the entire Southern Ocean.

6 Conclusions

Four XCTD sampling sections (November of 2012 and 2013; March of 2014 and 2015) from Fremantle, Australia to Antarctic Zhongshan Station and MODIS-A sea surface temperature products were used to study the structure and seasonal variability of the major fronts in the Southeast Indian Ocean.

Water mass analysis showed that the surface water masses (STSW, SASW and AASW) were less salty in March than in November. There was no obvious seasonal variability of SAMW.

The distribution of the major fronts identified by XCTD observation data agreed with previous studies, and the various fronts had different seasonal variabilities. The STF was southward by one degree in March compared with its location in November. The thermal front in March only existed in the upper 150-m layer, less than the depth of the saline front (~500 m). The structures of the two fronts were consistent in November. The gradient of the SAF was strong and its depth range was large. There was no seasonal change of SAF position. The saline front in the upper 100-m moved northward by about two degrees latitude in March, relative to the location in November. The PF location, identified by the northernmost extent of the 2°C isotherm, was stable, and the temperature gradient was ~1.4–2.0°C·(100 km)$^{-1}$. The SACCF location was 57°S–60°S in the sector 80°E–110°E.

MODIS-A SST products showed strong performance in the Southeast Indian Ocean. Seasonal variability of the major fronts along the 100°E section as identified by the surface layer temperature gradient was consistent with conclusions from the XCTD observations. The surface expression of the PF derived from the temperature gradient was southward by about one degree of latitude compared with its subsurface expression derived from the northernmost extent of the 2°C isotherm.

Acknowledgments The authors thank the Chinese Arctic and Antarctic Administration for supporting the field sampling. Special thanks go to the staff of *R/V XUE LONG* for supporting the XCTD data collection. This work was supported by the Chinese Polar Environment Comprehensive Investigation & Assessment Programs (Grant nos. CHINARE2012-2016 for 01-01-07, CHINARE2016-01-01, and CHINARE2016-04-01) and the National Natural Science Foundation of China (Grant nos. 41306206 and U1406404). We thank the editor and two anonymous reviewers for their helpful comments on the manuscript, special thanks to Dr. Robert Graham for the Southern Ocean digital fronts of Igor Belkin.

References

1 Talley L D, Pickard G L, Emery W J, et al. Descriptive physical oceanography: an introduction. 6th ed. Oxford, UK: Elsevier, 2011: 437–471
2 Orsi A H, Whitworth Ⅲ T, Nowlin Jr W D. On the meridional extent and fronts of the Antarctic Circumpolar Current. Deep Sea Res Part Ⅰ, 1995, 42(5): 641–673
3 Belkin I M, Gordon A L. Southern ocean fronts from the Greenwich meridian to Tasmania. J Geophys Res, 1996, 101(C2): 3675–3696
4 Rintoul S R, Bullister J L. A late winter hydrographic section from Tasmania to Antarctica. Deep Sea Res Part Ⅰ, 1999, 46(8): 1417–1454
5 Sokolov S, Rintoul S. Circulation and water masses of the southwest Pacific: WOCE Section P11, Papua New Guinea to Tasmania. J Mar Res, 2000, 58(2): 223–268
6 Sallée J B, Speer K, Morrow R. Response of the Antarctic circumpolar current to atmospheric variability. J Climate, 2008, 21(12): 3020–3039, doi: 10.1175/2007JCLI1702.1
7 Park Y H, Durand I, Kestenare E, et al. Polar front around the Kerguelen Islands: an up-to-date determination and associated circulation of surface/subsurface waters. J Geophys Res Ocean, 2014, 119(10): 6575–6592, doi: 10.1002/2014JC010061
8 Sokolov S, Rintoul S R. Structure of Southern Ocean fronts at 140°E. J Mar Syst, 2002, 37(1–3): 151–184, doi: 10.1016/S0924-7963(02)00200-2
9 Nagata Y, Michida Y, Umimura Y. Variation of positions and structures of the oceanic fronts in the Indian Ocean sector of the Southern Ocean in the period from 1965 to 1987//Sahrhage D. Antarctic ocean and resources variability. Berlin Heidelberg: Springer, 1988: 92–98
10 Yuan X J, Martinson D G, Dong Z Q. Upper ocean thermohaline structure and its temporal variability in the southeast Indian Ocean. Deep Sea Res Part Ⅰ, 2004, 51(2): 333–347
11 Shi J X, Zhao J P. Advances in Chinese studies on water masses, circulation and sea ice in the Southern Ocean (1995–2002). Adv Mar Sci, 2002, 20(4): 116–126 (in Chinese)
12 Gao G P, Han S Z, Dong Z Q, et al. Structure and variability of fronts in the South Indian Ocean along sections from Zhongshan Station to Fremantle. Acta Oceanol Sinica, 2003, 25(6): 9–19 (in Chinese)
13 He Z G, Dong Z Q, Hu J Y. Upper ocean hydrographic properties of Southeast Indian Ocean in Austral Summer, 2003. Chin J Polar Res, 2003, 15(3): 195–206 (in Chinese)
14 Gille S T. Mean sea surface height of the Antarctic Circumpolar Current from Geosat data: method and application. J Geophys Res, 1994, 99(C9): 18255–18273
15 Sokolov S, Rintoul S R. Multiple jets of the Antarctic circumpolar current South of Australia. J Phys Oceanogr, 2007, 37(5): 1394–1412, doi: 10.1175/JPO3111.1
16 Sokolov S, Rintoul S R. Circumpolar structure and distribution of the Antarctic Circumpolar Current fronts: 1. Mean circumpolar paths. J Geophys Res, 2009, 114(C11): C11018, doi: 10.1029/2008JC005108
17 Sokolov S, Rintoul S R. Circumpolar structure and distribution of the Antarctic Circumpolar Current fronts: 2. Variability and relationship to sea surface height. J Geophys Res, 2009, 114(C11), doi: 10.1029/2008JC005248
18 Billany W, Swart S, Hermes J, et al. Variability of the Southern Ocean fronts at the Greenwich Meridian. J Mar Syst, 2010, 82(4): 304–310, doi: 10.1016/j.jmarsys.2010.06.005
19 Graham R M, De Boer A M, Heywood K J, et al. Southern Ocean fronts: controlled by wind or topography?. J Geophys Res, 2012, 117(C8), doi: 10.1029/2012JC007887
20 Graham R M, De Boer A M. The dynamical subtropical front. J Geophys Res, 2013, 118(10): 5676–5685, doi: 10.1002/jgrc.20408
21 Kim Y S, Orsi A H. On the variability of Antarctic Circumpolar Current fronts inferred from 1992–2011 altimetry. J Phys Oceanogr, 2014, 44(12): 3054–3071, doi: 10.1175/JPO-D-13-0217.1
22 Legeckis R. Oceanic polar front in the drake passage-satellite observations during 1976. Deep Sea Res, 1977, 24(7): 701–704
23 Lutjeharms J R E, Valentine H R. Southern Ocean thermal fronts south of Africa. Deep Sea Res Part A, 1984, 31(12): 1461–1475
24 Moore J K, Abbott M R, Richman J G. Variability in the location of the Antarctic Polar Front (90°-20°W) from satellite sea surface temperature data. J Geophys Res, 1997, 102(C13): 27825–27833
25 Moore J K, Abbott M R, Richman J G. Location and dynamics of the Antarctic polar front from Satellite Sea surface temperature data. J Geophys Res, 1999, 104(C2): 3059–3073
26 Kostianoy A G, Ginzburg A I, Frankignoulle M, et al. Fronts in the Southern Indian Ocean as inferred from satellite sea surface temperature data. J Mar Syst, 2004, 45(1–2): 55–73, doi: 10.1016/j.jmarsys.2003.09.004
27 Dong S F, Sprintall J, Gille S T. Location of the Antarctic polar front from AMSR-E satellite sea surface temperature measurements. J Phys Oceanogr, 2006, 36(11): 2075–2089
28 Dong S F, Gille S T, Sprintall J, et al. Validation of the advanced microwave scanning radiometer for the earth observing system (AMSR-E) sea surface temperature in the Southern Ocean. J Geophys Res, 2006, 111(C4): C04002, doi: 10.1029/2005JC002934
29 Freeman N M, Lovenduski N S. Mapping the Antarctic Polar Front: weekly realizations from 2002 to 2014. Earth Syst Sci Data, 2016, 8(1): 191–198, doi: 10.5194/essd-8-191-2016
30 Freeman N M, Lovenduski N S, Gent P R. Temporal variability in the Antarctic Polar Front (2002–2014). J Geophys Res: Oceans, 2016, 121, doi: 10.1002/2016JC012145
31 Park Y H, Camberoni L, Charriaud E. Frontal structure, water masses, and circulation in the Crozet Basin. J Geophys Res, 1993, 98(C7): 12361–12385
32 Whitworth Ⅲ T, Orsi A H, Kim S J, et al. Water masses and mixing near the Antarctic slope front//Jacobs S S, Weiss R F. Ocean, ice, and atmosphere: interaction at the Antarctic continental margin Antarctic research series. Washington, DC: AGU, 2013: 1–27
33 Pollard R T, Lucas M I, Read J F. Physical controls on biogeochemical zonation in the Southern Ocean. Deep Sea Res Part II, 2002, 49(16): 3289–3305, doi: 10.1016/S0967-0645(02)00084-X